International Journal of Nanomedicine

Dovepress
open access to scientific and medical research

Open Access Full Text Article

ORIGINAL RESEARCH

Characterization of Silver Nanoparticles Synthesized by Leaves of *Lonicera japonica* Thunb

Yu Zhang[1–3,*], Li Cui[2,*], Yizeng Lu[4], Jixiang He[5], Hidayat Hussain[6], Lei Xie[4], Xuan Sun[2], Zhaoqing Meng[7], Guiyun Cao[7], Dawei Qin[1], Daijie Wang[2,3]

[1]School of Chemistry and Chemical Engineering, Qilu University of Technology (Shandong Academy of Sciences), Jinan, 250353, People's Republic of China; [2]School of Pharmaceutical Sciences and Key Laboratory for Applied Technology of Sophisticated Analytical Instruments of Shandong Province, Shandong Analysis and Test Center, Qilu University of Technology (Shandong Academy of Sciences), Jinan, 250014, People's Republic of China; [3]Biological Engineering Technology Innovation Center of Shandong Province, Heze Branch of Qilu University of Technology (Shandong Academy of Sciences), Heze, 274000, People's Republic of China; [4]Shandong Provincial Center of Forest and Grass Germplasm Resources, Jinan, 250102, People's Republic of China; [5]School of Pharmacy, Shandong University of Traditional Chinese Medicine, Jinan, 250353, People's Republic of China; [6]Department of Bioorganic Chemistry, Leibniz Institute of Plant BioChemistry, Halle, D-06120, Germany; [7]Shandong Hongjitang Pharmaceutical Group Co., Ltd., Jinan, 250103, People's Republic of China

*These authors contributed equally to this work

Correspondence: Dawei Qin, School of Chemistry and Chemical Engineering, Qilu University of Technology (Shandong Academy of Sciences), Jinan, 250353, People's Republic of China, Tel/Fax +86 53189631208, Email qdw@qlu.edu.cn; Daijie Wang, Biological Engineering Technology Innovation Center of Shandong Province, Heze Branch of Qilu University of Technology (Shandong Academy of Sciences), Heze, 274000, People's Republic of China, Tel +86 53182605319, Fax +86 53182964889, Email wangdaijie@qlu.edu.cn

Background: The leaves of *L. japonica* (LLJ) are widely used as medicine in China. It is rich in caffeoylquinic acids, flavonoids and iridoid glycosides and has strong reducing capacities. Therefore, it can be used as a green material to synthesize silver nanoparticles.
Methods: LLJ was used as a reducing agent to produce the LLJ-mediated silver nanoparticles (LLJ-AgNPs). The structure and physicochemical properties of LLJ-AgNPs were characterized by ultraviolet spectroscopy (UV-Vis), scanning electron microscopy (SEM), transmission electron microscopy (TEM), Fourier transform infrared spectroscopy (FTIR), and x-ray powder diffraction (XRD). Antioxidant activity of LLJ-AgNPs was determined by 1,1-diphenyl-2-picrylhydrazyl (DPPH) scavenging. Antibacterial activity was determined by 96 well plates (AGAR) gradient dilution, while the anticancer potential was determined by MTT assay.
Results: The results showed LLJ-AgNPs had a spherical structure with the maximum UV-Vis absorption at 400 nm. In addition, LLJ-AgNPs exhibited excellent antioxidant properties, where the free radical scavenging rate of LLJ-AgNPs was increased from 39% to 92% at concentrations from 0.25 to 1.0 mg/mL. Moreover, LLJ-AgNPs displayed excellent antibacterial properties against *E. coli* and *Salmonella* at room temperature, with minimum inhibitory values of 10^{-6} and 10^{-5} g/L, respectively. In addition, the synthetic LLJ-AgNPs exhibited a better inhibition effect in the proliferation of cancer cells (HepG2, MDA-MB −231, and Hela cells).
Conclusion: The present study provides a green approach to synthesize LLJ-AgNPs. All those findings illustrated that the produced LLJ-AgNPs can be used as an economical and efficient functional material for further applications in food and pharmaceutical fields.
Keywords: leaves of *Lonicera japonica* Thunb, LLJ-$AgNO_3$-NPs, green approach, antioxidant, antibacterial, anticancer

Introduction

In recent years, more and more researchers have shifted their research focus to functional natural products, such as Coptis Chinensis Franch, Forsythia Suspense (Thunb.) Vahl, and *Lonicera japonica* Thunb, due to their excellent functionalities such as anti-oxidant, anti-bacterial, and anti-cancer effects.[1–6] The Leaves from *L. japonica* (LLJ) are traditionally used as medicine in Asian countries. It is rich in caffeoylquinic acids, flavonoids and iridoid glycosides, which have antioxidant, antivirus, antibacterial and other functional properties[7–12] Nanoparticles (NPs) are widely used in biology, medicine, electrical, and chemical industries.[13] The interest in using metal colloids as nanocarriers has been growing as their structure can be modified by introducing specific functional groups.[14] The performance of NPs can be controlled by two parameters: size and shape.[15] Silver nanoparticles (AgNPs) are fine particles of metallic silver ranging in size from 1

Received: 3 January 2022
Accepted: 24 March 2022
Published: 6 April 2022

to 100 nm. They are versatile nanomaterials and have excellent functional properties, such as antimicrobial, antifungal, and anti-inflammatory capacities.[16]

Although there are many ways to synthesize nanoparticles, research about the green synthesis method has become a hot topic in recent years.[17,18] A variety of reducing agents, including biomass, plant extracts,[19,20] microorganisms,[21] have been used in green synthesis research.[22] Among those reducing agents, biomass, especially flavonoids, was considered one of the most effective compounds to reduce Ag^+ to AgNPs. More importantly, flavonoids are present widely in almost all plants, which indicates they are economically available and sustainable.

The current research aims to develop a green and innovative method to produce AgNPs using LLJ extract as a reducing agent. The structural and physicochemical properties of produced AgNPs were characterized using ultraviolet spectroscopy (UV-Vis), scanning electron microscopy (SEM), transmission electron microscopy (TEM), Fourier transform infrared spectroscopy (FTIR), and X-ray powder diffraction (XRD). Moreover, the functional properties of AgNPs, including anti-oxidant, anti-bacterial, and anti-cancer properties, were investigated in this study.

Materials and Methods

Materials

The leaves of LLJ were collected in Linyi, Shandong Province, and identified by Prof. Jixiang He (College of Pharmacy, Shandong University of Traditional Chinese Medicine). A voucher specimen (20180701006) has been deposited at the Shandong Analysis and Test Centre. All chemicals, including trifluoroacetic acid, trimethylamine, 2,2-Diphenyl-1-pyridine hydrazide (DPPH), butylated hydroxytoluene (BHT), silver nitrate for AgNPs synthesis, and anhydrous were analytical grade and purchased from Sinopharm Chemical Reagent Co., Ltd (Shanghai, China). All aqueous solutions were prepared using deionized water produced by the Milli-Q osmosis system (Millipore, USA). HeLa cell lines were bought from the American Type Culture Collection. HepG2 cell lines were purchased from the Shanghai Gefan Biotechnology Co., Ltd (GF589). MDA-MB-231 cells were obtained from the Nanjing Cobioer Biosciences Co., Ltd (CBP60382).

Apparatus

The FTIR results were determined and analyzed using Nicolet 710 FTIR spectrometer (Thermo Fisher, USA). The metal composition of the nanoparticles was determined using IRIS Advantage OPTIMA 7000DV inductively coupled plasma atomic emission spectrometer (Thermo Perkin-Elmer). Surface morphology, particle size, and microstructure of the NPs were determined using a SUPRA™ 55 Thermal Field Emission Scanning Electron Microscopy (Carl Zeiss, Germany). The transmission electron microscopy images of the NPs were acquired using a JEM-2100F transmission electron microscope (JEOL, Japan). X-ray diffraction studies were performed using an EMPYREAN X-ray diffractometer (PANalytical, The Netherlands). A Genesys 10S UV-vis spectrometer (Thermo Fisher) was used for ultraviolet and visible spectral analysis.

Preparation of LLJ Extracts

Fifty grams of the dried LLJ were crushed into powder and added to 500 mL 75% ethanol solution. The samples were extracted using ultrasonication at 50°C for 40 minutes to obtain the crude extract. The obtained sample solution was then extracted three times with isometric petroleum ether. The remaining aqueous solution was freeze-dried. Finally, 12.6 g of crude LLJ extracts were obtained with a yield of 25.2% (*w*/*w*).

Synthesis of Silver Nanoparticles

The freeze-dried LLJ extracts (20 mg) were dissolved in 9 mL of deionized water and then mixed with $AgNO_3$ solution, which was then placed in an oil bath at a temperature of 60 °C and maintained for 24 h for complete reaction. After that, the produced suspension was centrifuged at 8000 rpm for 30 minutes. The concentration of Ag^+ in the supernatant, which represented unconverted Ag, was determined by ICP. The precipitated AgNPs were washed three times using deionized water to remove the excess organics and stored in the refrigerator for further use.

Reaction Condition Optimization for Biosynthesis

The optimal conditions for AgNPs biosynthesis were determined by changing the concentration of LLJ, pH, and temperature. Nine mL of LLJ solution with different concentrations was mixed with 1 mL $AgNO_3$ solution (1mL) to achieve the final LLJ concentrations of 8, 10, 15, and 20 mg/mL, respectively. Trifluoroacetic acid and triethylamine were used to adjust the pH values to 2, 4, 6, 8, and 10. For the determination of the optimum reaction temperature, different temperatures (40, 50, 60, and 70°C) were used to produce the nanoparticles.

Characterization of Silver Nanoparticles

Ultraviolet-Visible Spectroscopy

Surface plasmon resonance (SPR) peaks of formed AgNPs nanoparticles were monitored using a UV-Vis spectrophotometer (UV-Vis spectra). Aliquots of the samples (AgNPs diluted with distilled water) were poured into a 1.0 cm cell, and then the UV-Vis spectra were recorded in the wavelength range of 330–800 nm. All experiments were performed at room temperature (25°C).

SEM, TEM, FTIR, XRD, and XPS Analysis

Scanning electron microscopic analysis (SEM) was used to observe the microstructure of AgNPs at different magnifications. Images of the AgNPs were acquired using a Quanta 200FEG SEM spectrometer at 20 kV, 10 mA, SE mode, and spot size 3.5 (Hillsboro, OR, USA). The xerogel was coated with a thin layer of gold by sputtering before observation. After dropping a thin layer of AgNPs on a carbon-coated copper grid, the size and morphology of silver nanoparticles of the sample were observed for 5 minutes under a mercury lamp.

Transmission electron micrographs of AgNPs were taken using a Tecnai G2 20 TWIN transmission electron microscope (Hillsboro) with a copper mesh as support. Rheological measurements were performed using a Kinexus pro+ rheometer (Malvern, UK) equipped with a temperature controller and parallel stainless steel plates (20 mm diameter, 0.5 mm spacing). After shaking, the gel was placed in the shear gap of the rheometer and incubated at 15°C. It was then subjected to a frequency sweep or stress sweep for testing.

Fourier transform infrared spectroscopy (FTIR) was applied in the wavelength range between 4000 and 400 cm^{-1} to determine the functional groups in the synthesized AgNPs. The AgNPs were dried, ground with KBr pellets, and analyzed. X-ray powder diffraction (XRD) was performed by immersing a glass plate containing a thin film of the AgNPs in a solution.

The structure of the synthesized AgNPs was determined by X-ray photoelectron spectroscopy (XPS). The AgNPs were compacted and then vacuumed for testing.

Conversion of Ag+ Ions

The synthesized AgNP suspensions were centrifuged at 8000 rpm for 30 min, and the residual Ag^+ was separated from the generated AgNPs. The concentration of Ag^+ in the supernatant represented the residual or unconverted concentration of Ag^+ was determined using ICP. The converted Ag+ was calculated using total Ag^+ to subtract the unconverted Ag^+. The conversion rate of Ag^+ was determined by dividing original Ag+ with unconverted Ag^+.

Antioxidant Activity of AgNPs

The antioxidant activity of the synthesized nanoparticles was determined by scavenging free radicals from DPPH.[23,24] The DPPH (0.015 μg/mL) solution was prepared by dissolving in anhydrous ethanol, and then mixed with AgNPs solutions to achieve final concentrations of 0.01, 0.25, 0.5, 0.75, and 1.0 mg/mL, which were then mixed and reacted at 30°C for 30 minutes. The absorbance of each test tube was determined using an ultraviolet-visible spectrometer at 517 nm. Butylated hydroxytoluene (BHT) was used as a positive control and the sample containing only DPPH was used as blank. The DPPH radical scavenging activity was calculated using the following equation. DPPH scavenging effect (%) = $[(A_0 - A_t)/A_0] \times 100$

where A_0 is the absorbance of the control and A_t is the absorbance of the sample.

Antibacterial Activity of AgNPs

The antibacterial activity of AgNPs was determined by measuring their inhibition effect against human pathogenic microorganisms *E. coli* and *Salmonella*. The MIC was determined by gradient dilution in 96-well plates. AgNPs were mixed with bacterial fluids at different ratios. After adding normal saline to the cultured cells for 24 hours, a certain amount of the liquid was taken from the mixture and evenly applied to the AGAR plate containing the nutrient broth. After cultivation at 37°C for 24 hours, the withdrawal on the plate was counted, which was used to generate the intuitive curve of bacterial inhibition rate. All experiments were performed under aseptic conditions.

Anticancer Activity of AgNPs

Hela, HepG2, and MDA-MB-231 cells were seeded in 96-well plates with 5000 cells per well and incubated for 48 hours. After that, aliquots of 10 μL of MTT solution (5 mg/mL) were added and incubated at 37°C for another 4 hours. Then the medium was aspirated, and the wells were washed with PBS. Meanwhile, aliquots of 150 μL DMSO were added to each well. The dye was dissolved by placing it on a shaker until the complete dissolution of formazan crystals. A microplate reader was used to determine the absorbance spectrophotometrically at 490 nm. The inhibition value was calculated using the following formula.

$$\text{Inhibition (\%)} = (\text{OD}_{\text{value of control well at 490 nm}} - \text{OD}_{\text{value of sample well at 490 nm}})/(\text{OD}_{\text{value of control well at 490 nm}} - \text{OD}_{\text{value of blank well at 490 nm}})$$

Results and Discussion

Determination of Optimum Production Conditions of AgNPs

Figure 1A and B show the influence of the concentration of LLJ extract on AgNP synthesis. As shown, Ag^+ concentration was 35.65% and 41.67% at the LLJ concentrations of 8 and 10 mg/mL, indicating poor conversion of Ag^+ into nanoparticles. Further increase of the concentration of LLJ to 15 mg/mL significantly increased UV absorption value and resulted in a higher Ag^+ conversion rate of 56.37%. The highest silver ion conversion rate value of 68.34% was observed at the concentration of 20 mg/mL, where the absorption peak was narrower and more stable Therefore, 20 mg/mL was selected for the production of AgNPs.

Figure 1C and D show the effect of temperature on AgNPs synthesis (40, 50, 60, and 70°C). At 40 and 50°C, the absorption peak was relatively broad, and the conversion rates were low (50.12% and 56.13%), which indicated that these two temperatures were not suitable for AgNPs synthesis. At the highest temperature of 70°C, the conversion rate of silver ions increased to 71.7%. However, the peak was broad, indicating a negative influence on the formation of nanoparticles. By contrast, the absorption peak at 60°C was narrow and stable, indicating the production of more homogeneous nanoparticles. Moreover, the silver ion conversion rate was also high with a value of 70.8%.

Figure 1E and F show the influence of pH on the formation of AgNPs. At alkaline conditions, unstable nanoparticles were formed as the absorption spectra were broad although the conversion rate of silver ions was high. Similarly, relative broad adsorption spectra were observed at pH 6.0 although almost all silver ions were converted into nanoparticles. Further decrease of pH to 4 reduced the conversion rate of silver ions to 71.67%. However, the produced AgNPs had sharp and narrow ultraviolet absorption peaks, demonstrating the formation of stable nanoparticles. Therefore, pH 4.0 was selected for the production of AgNPs in the following research.

Characterization of Produced AgNPs

Figure 2 shows the morphology and size of the synthesized AgNPs with LLJ extracts. As shown in the SEM image (Figure 2A), AgNPs were present as dotted circular particles with sizes between 20 to 50 nm. Further observation using TEM showed that AgNPs had a spherical structure and a similar biological membrane (Figure 2B). In addition, the particle size of AgNPs, in this case, was found to be between 50–200 nm.

FTIR was used to identify the bonds and functional bonds between LLJ extracts and Ag^+, which is critical to understanding their involvement in the reduction process. As summarized in Figure 2C, four major peaks were obtained for AgNPs. The peaks at 3410 are attributed to the stretching vibration of υ (O-H) and the in-plane bending vibration of δ

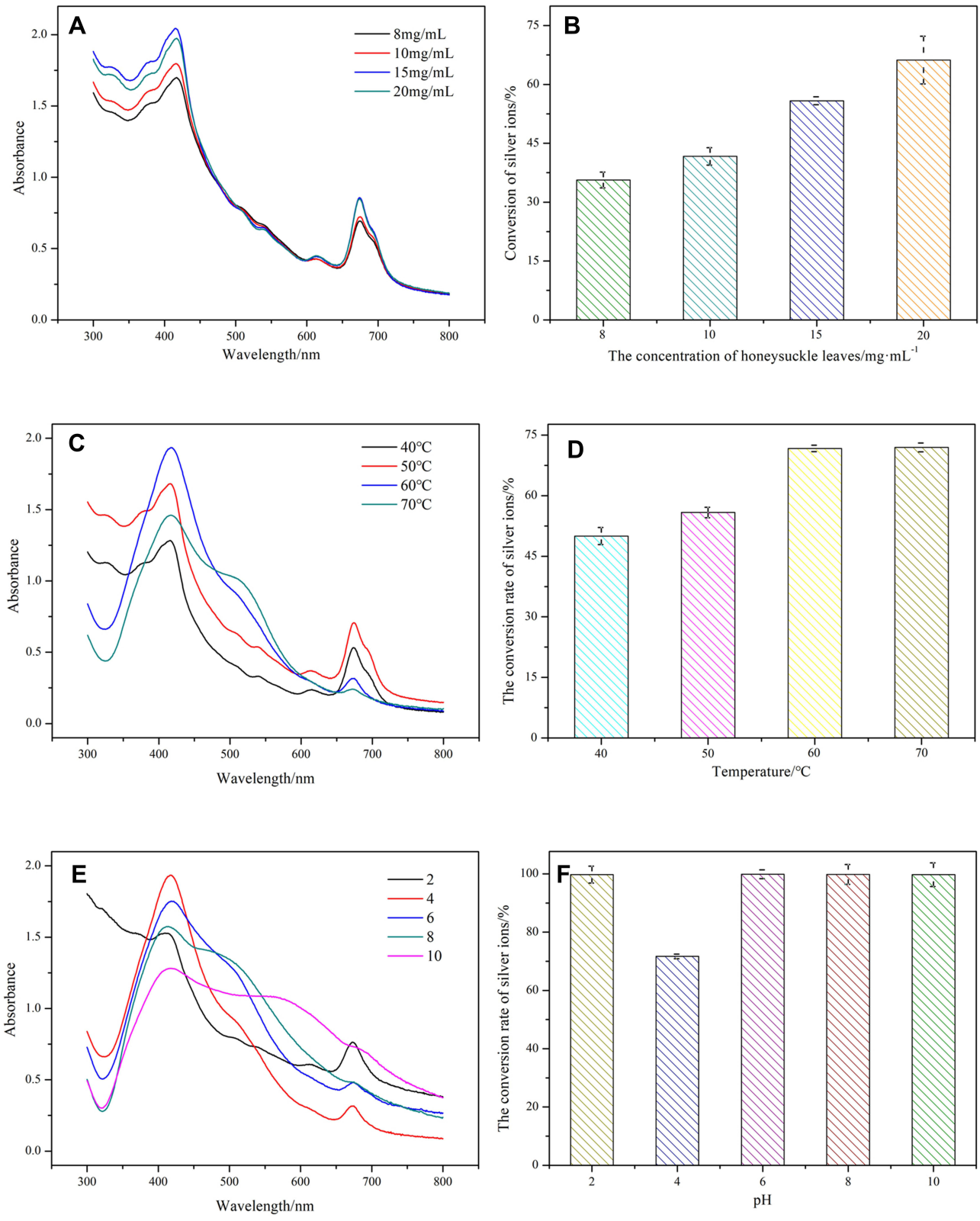

Figure 1 (**A**) UV–Vis spectra of AgNPs synthesized by LLJ at different Ag^+ concentrations; (**B**) Silver ion conversion rate of AgNPs synthesized by LLJ at different Ag^+ concentrations; (**C**) UV–Vis spectra of AgNPs synthesized by LLJ at different pH; (**D**) Silver ion conversion rate of AgNPs synthesized by LLJ at different pH; (**E**) UV–Vis spectra of AgNPs synthesized by LLJ at different temperatures; (**F**) Ag conversion rate of AgNPs synthesized by LLJ at different temperatures.

Abbreviations: UV–Vis spectra, UV-Vis spectrophotometer; LLJ, leaves of *L. japonica*; AgNPs, AgNPs, silver nanoparticles.

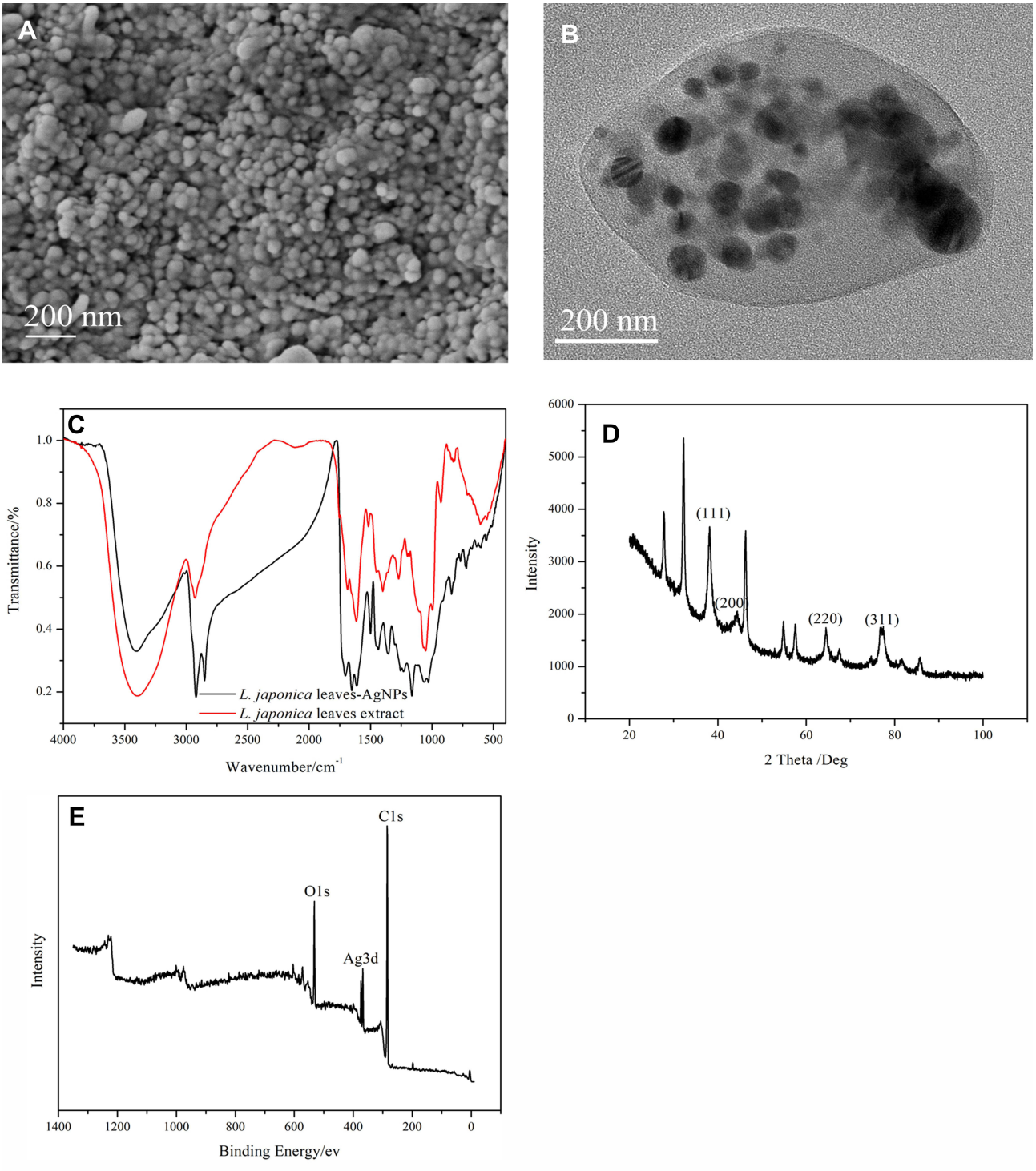

Figure 2 (**A**) SEM image of AgNPs synthesized by LLJ; (**B**) TEM image of AgNPs synthesized by LLJ; (**C**) FTIR image of AgNPs synthesized by LLJ; (**D**) XRD pattern of AgNPs synthesized by LLJ; (**E**) XPS pattern of AgNPs synthesized by LLJ.

Abbreviations: SEM, scanning electron microscopy; AgNPs, silver nanoparticles; LLJ, leaves of *L. japonica*; TEM, transmission electron microscopy; FTIR, Fourier transform infrared spectroscopy; XRD, x-ray powder diffraction; XPS, x-ray photoelectron spectroscopy.

(O-H). The absorption at 1610 cm^{-1} can be attributed to the stretching vibration of υ (=C-H) and υ (C=C).[25] The peak at 1610 cm^{-1} could also be related to the water molecule adsorbed on the surface. In addition, the peak at 1090 cm^{-1} could be attributed to the skeletal C-O and C-C vibrational bands of the glycosides.[26] All those peaks indicated the presence of residual flavonoids from LLJ extract on the surface of the obtained AgNPs.

Figure 2D shows the XRD results of the synthesized AgNPs. The narrow peaks indicate the crystalline properties of the nanoparticles. Four intense peaks corresponding to the 2θ values of 38.14°, 44.33°, 64.47°, and 77.42° were detected, which represent the face-centered cubic (fcc) lattice of silver with Miller indices of (111), (200), (220), and (311), respectively. From the peak intensity ratio of (111) compared to other diffraction peaks, it can be concluded that the (111) plane was the predominant orientation in the silver crystal structure of the biosynthesized AgNPs.

Figure 2E shows the XPS full spectrum of the synthesized AgNPs. The main elements in the AgNPs were C, O, and Ag, which further demonstrated the presence of LLJ on the surface of the silver nanoparticles.

Antioxidant Activity

The radical scavenging activity of AgNPs was determined by the 2.2-Diphenyl-1-pyridine hydrazide (DPPH) method. As shown in Figure 3, the radical scavenging activity of AgNPs increased steadily from 39.12% to 92.36%, with increasing LLJ concentration from 0.25 to 1mg/mL. At high LLJ concentrations, the radical scavenging activity of LLJ-AgNPs was similar to that of BHT (positive control). LLJ was reported to possess the ability to reduce $DPPH^{+}$ and $ABTS^{+}$.[7,8] The present results further proved that the antioxidant capacity of LLJ extracts can be enhanced in the form of LLJ-AgNPs.

Antibacterial Activity

The inhibition of AgNPs on the growth of bacteria was also investigated in this research. As shown, the minimum inhibitory concentrations (MIC) of AgNPs on *Escherichia coli* (*E. coli*) and *Salmonella* were 10^{-6} and 10^{-5} g/L, respectively, indicating that the synthetic LLJ-AgNPs had a sufficient inhibitory effect on both bacteria (Figure 4).

From the curves of inhibition rate of *E. coli* and *Salmonella* (Figure 5), it was found that the inhibition rate increased with the increasing concentration of the sample. Furthermore, LLJ-AgNPs exhibited a better antibacterial effect compared to LLJ and tetracycline. Further observation using a bacterial electron microscope indicated that the AgNPs could partially damage the structure and morphology of bacteria, which prevented the growth and multiplication of bacteria (Figure 6). LLJ has been reported for its ideal and potent antibacterial activity on *E. coli, Staphylococcus aureus,*

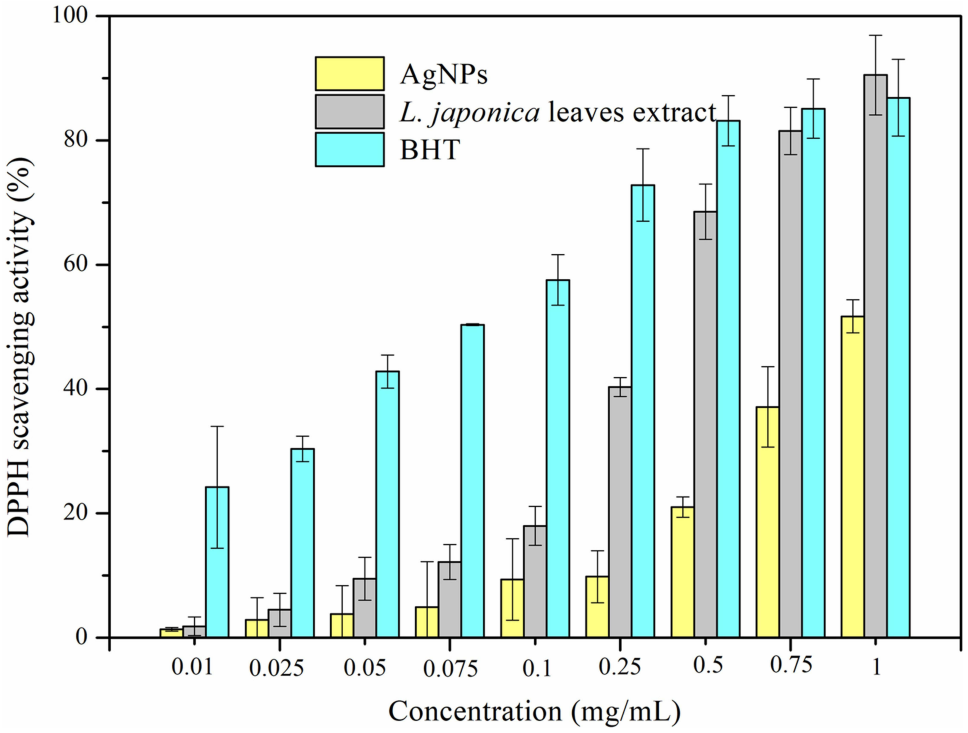

Figure 3 Comparison of free radical DPPH clearance rate between AgNPs, LLJ, and BHT.
Abbreviations: DPPH, 1,1-diphenyl-2-picrylhydrazyl; AgNPs, silver nanoparticles; LLJ, leaves of *L. japonica*; BHT, butyl hydroxy toluene.

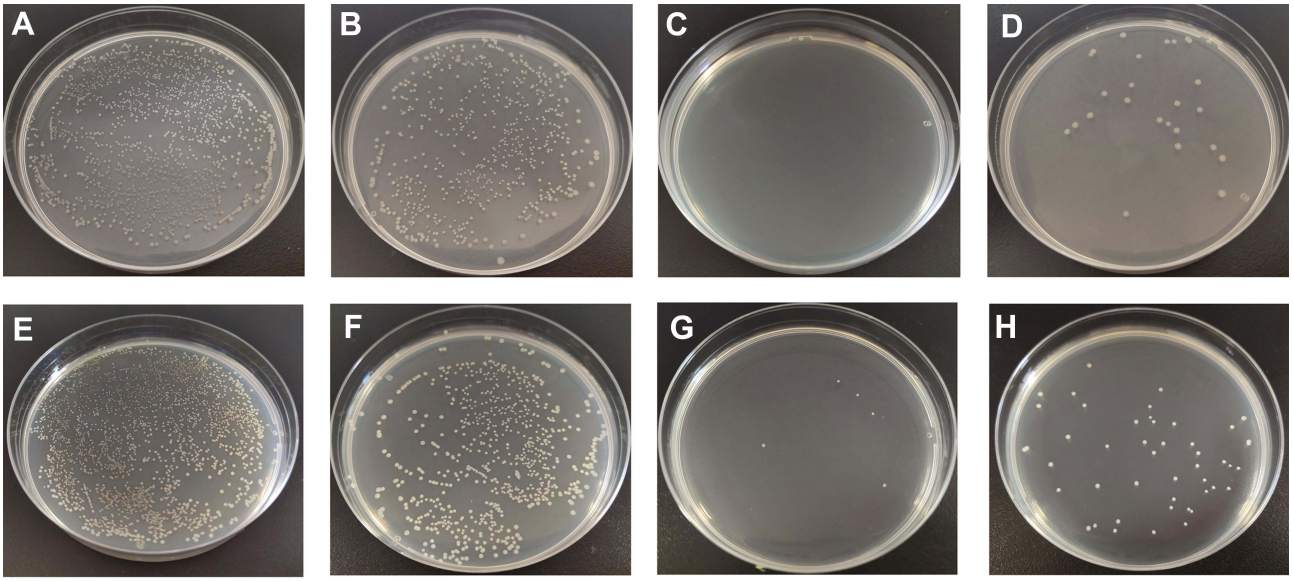

Figure 4 Amount of viable bacteria of culture medium. (**A**) *E. coli*; (**B**) *E. coli* treated with 0.1 mg/mL LLJ; (**C**) *E. coli* treated with 0.1 mg/mL AgNPs; (**D**) *E. coli* treated with 0.1 mg/mL tetracycline; (**E**) *Salmonella*; (**F**) *Salmonella* treated with 0.1 mg/mL LLJ; (**G**) *Salmonella* treated with 0.1 mg/mL AgNPs; (**H**) *Salmonella* treated with 0.1 mg/mL tetracycline.
Abbreviations: *E. coli, Escherichia coli*; LLJ, leaves of *L. japonica*; AgNPs, silver nanoparticles.

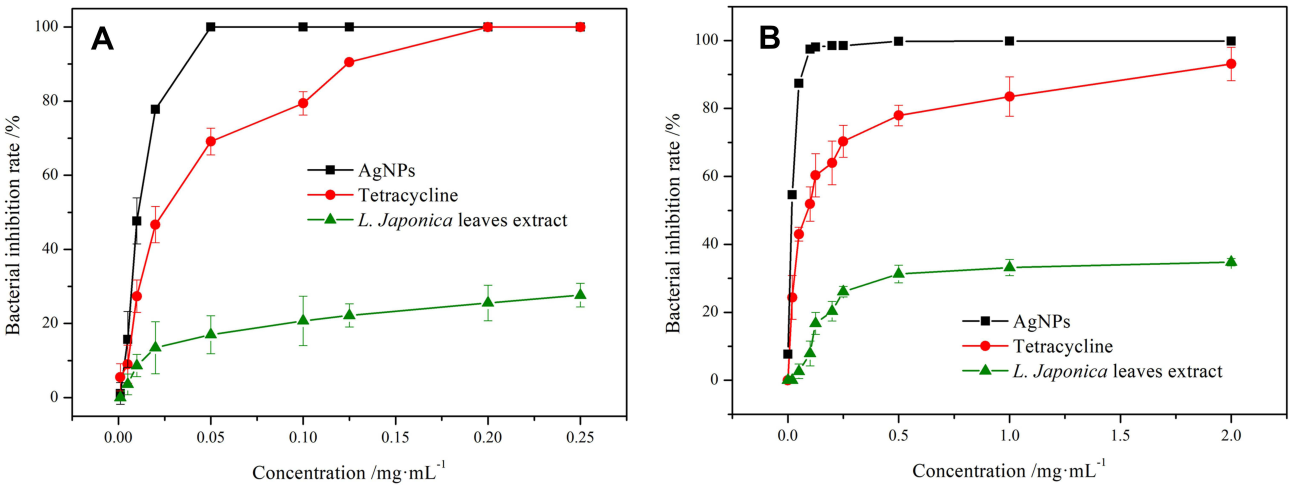

Figure 5 The inhibition rate curves of different samples to bacteria. (**A**). *E. coli*; (**B**). *Salmonella.*
Abbreviation: *E. coli, Escherichia coli.*

Bacillus subtilis, Salmonella typhimurium, Penicillium notatum, Aspergillus niger, Aspergillus flavus, and *Saccharomyces cerevisiae*.[27,28] The LJJ-mediated AgNPs could also provide an economical and better alternative for its inhibitory potential against food-borne bacteria.

Anticancer Activity

The anticancer activity of LLJ-AgNPs was determined against several cancer lines, including cervical cancer (Hela), liver cancer (HepG2), and breast cancer (MDA-MB-231) using the MTT assay at different concentrations (Figure 7A–C). As expected, the synthetic LLJ-AgNPs showed better biocompatibility than LLJ in all cell lines. For Hale, the LLJ-AgNPs showed better activity even at low concentrations, and the activity further increased with increasing concentration. LLJ alone did not significantly inhibit the proliferation of HepG2 cells. However, the inhibitory effect became more evident

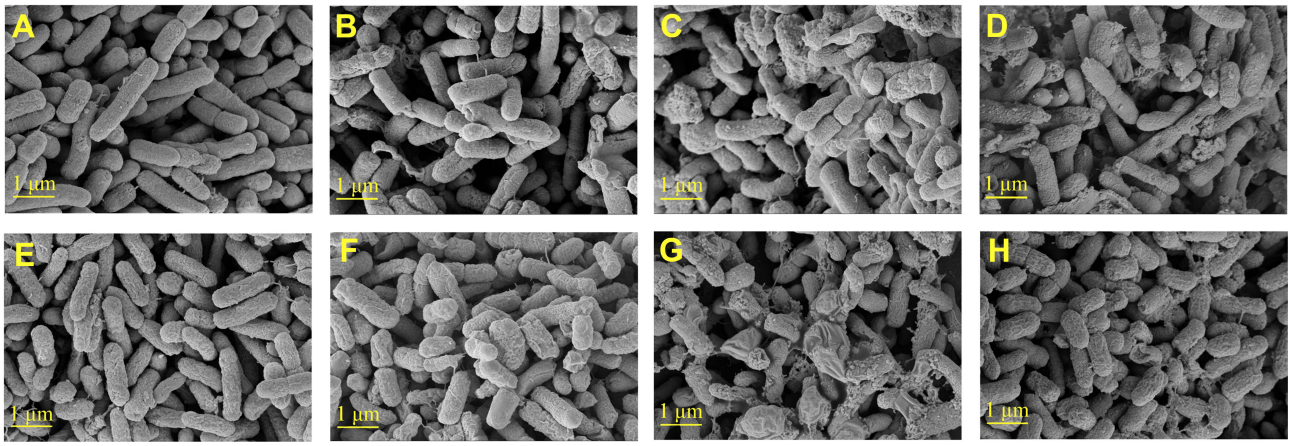

Figure 6 SEM images of bacterial morphology. (**A**) *E. coli*; (**B**) *E. coli* with LLJ; (**C**) *E. coli* with AgNPs; (**D**) *E. coli* with tetracycline; (**E**) *Salmonella*; (**F**) *Salmonella* with LLJ; (**G**) *Salmonella* with AgNPs; (**H**) *Salmonella* with tetracycline.
Abbreviations: *E. coli, Escherichia coli*; LLJ, leaves of *L. japonica*; AgNPs, silver nanoparticles.

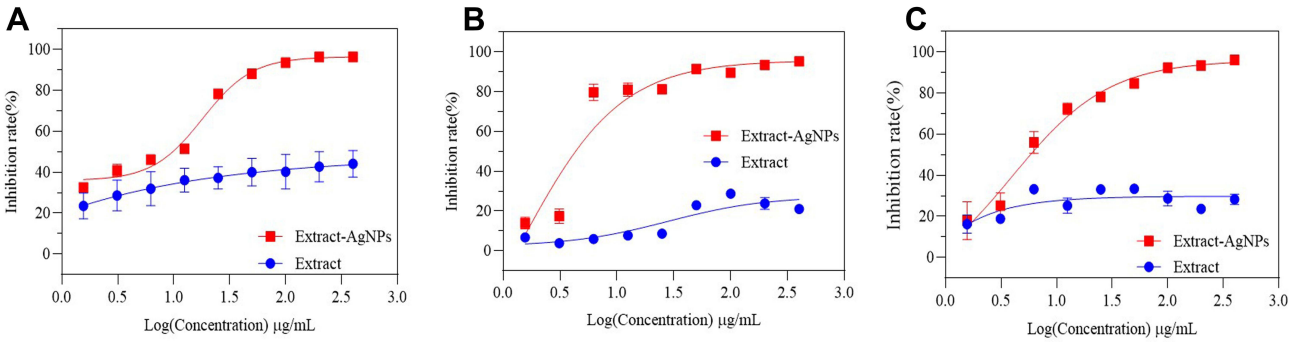

Figure 7 The inhibition rate curves of AgNPs to different cancer cell lines. (**A**) Hela; (**B**) HepG2; (**C**) MDA-MB-231.
Abbreviations: AgNPs, silver nanoparticles; HeLa, human cervical cancer cell line; HepG2, human hepatoma cancer cell line; MDA-MB-231, breast adenocarcinoma cell line.

after it was used in the form of LLJ-AgNPs, indicating that nanoparticles improved the anticancer activity of LLJ against HepG2 cells. A similar phenomenon has been observed for the inhibitory effect of LLJ-AgNPs on MDA-MB-231 cells.

Previously, components in *Lonicera japonica* showed strong anti-cancer activities. The anticancer activities were performed through the induction of apoptosis and against H2O2-induced injury in cells ($p < 0.001$).[29–31] These results indicated that the components in LLJ could be served as functional food for anti-cancer activity. The nanonization of LLJ, as proved in the present study, thus further enhances the anticancer activity, and it provides better chances for clinical trials.

Conclusion

Developing a biosynthetic method of AgNPs with high efficiency, environment friendly, and lower cost is essential in current nanotechnology research and application. The present study demonstrated that the extract of *L. japonica* leaves could be used to produce AgNPs with improved functionalities. The optimum produce conditions are found to be at LLJ concentration of 20 mg/mL, 60°C, and pH 4.0. The produced AgNPs have a spherical structure and homogeneous size distribution of moderate size. Moreover, the biosynthesized AgNPs exhibited a significant inhibition effect against the growth of *E. coli* and *Salmonella*. They also showed remarkable inhibitory activity against three cancer cell types HepG2, MDA-MB-231, and Hela. All those results indicated that it is feasible to produce functional silver nanoparticles through the reducing effect of LLJ extract. The produced AgNPs have a stable structure that can be potentially used as nanocarriers for future applications.

Acknowledgments

We gratefully acknowledge the Science, Education and Industry Integration Innovation Pilot Project from Qilu University of Technology (Shandong Academy of Sciences) (2020KJC-GH08), the Subject of Key R&D plan of Shandong Province (Agricultural Elite Varieties Project) (2020LZGC0090301), Quancheng Industry Leading Talent Program in Jinan and "Double-Hundred Talent Plan" program from Shandong Province.

Disclosure

Zhaoqing Meng and Guiyun Cao are employees of Shandong Hongjitang Pharmaceutical Group Co., Ltd. The authors report no other potential conflicts of interest in this work.

References

1. Zhang J, Wang YZ, Yang WZ, Yang MQ, Zhang JY. Research progress in chemical constituents in plants of Polygonatum and their pharmacological effects. *Zhongguo Zhong Yao Za Zhi*. 2019;44(10):1989–2008. doi:10.19540/j.cnki.cjcmm.20190222.006
2. Yu L, Gan X, Zhou D, He F, Zeng S, Hu D. Synthesis and antiviral activity of novel 1,4-pentadien-3-one derivatives containing a 1,3,4-thiadiazole moiety. *Molecules*. 2017;22(4):658. doi:10.3390/molecules22040658
3. Meng X, Tang GY, Liu PH, Zhao C, Liu Q, Li H. Antioxidant activity and hepatoprotective effect of 10 medicinal herbs on CCl4-induced liver injury in mice. *World J Gastroenterol*. 2020;26(37):5629–5645. doi:10.3748/wjg.v26.i37.5629
4. Wang K, Chen Q, Shao Y, et al. Anticancer activities of TCM and their active components against tumor metastasis. *Biomed Pharmacother*. 2021;133:111044. doi:10.1016/j.biopha.2020.111044
5. Long SF, He TF, Wu D, Yang M, Piao XS. Forsythia suspensa extract enhances performance via the improvement of nutrient digestibility, antioxidant status, anti-inflammatory function, and gut morphology in broilers. *Poult Sci*. 2020;99(9):4217–4226. doi:10.1016/j.psj.2020.05.011
6. Liu J, Lin L, Jia Z, et al. Antibacterial potential of Forsythia suspensa polysaccharide against resistant Enterobacter cloacae with SHV-12 extended-spectrum β-lactamase (ESBL). *J Cell Mol Med*. 2020;24(15):8763–8771. doi:10.1111/jcmm.15510
7. Seo ON, Kim GS, Park S, et al. Determination of polyphenol components of Lonicera japonica Thunb. using liquid chromatography-tandem mass spectrometry: contribution to the overall antioxidant activity. *Food Chem*. 2012;134(1):572–577. doi:10.1016/j.foodchem.2012.02.124
8. Wang D, Du N, Wen L, et al. An efficient method for the preparative isolation and purification of flavonoid glycosides and caffeoylquinic acid derivatives from leaves of *Lonicera japonica* Thunb. using high-speed counter-current chromatography (HSCCC) and prep-HPLC guided by DPPH-HPLC experiments. *Molecules*. 2017;22(2):229. doi:10.3390/molecules22020229
9. Li RJ, Kuang XP, Wang WJ, Wan CP, Li WX. Comparison of chemical constitution and bioactivity among different parts of *Lonicera japonica* Thunb. *J Sci Food Agric*. 2020;100(2):614–622. doi:10.1002/jsfa.10056
10. Lin D, Zhao G, Liu J. Extraction of active components from Flos Lonicerae and their bacteriostatic test. *Nat Prod Res Dev*. 2003;15:436–437. doi:10.16333/j.1001-6880.2003.05.017
11. Rahman A, Kang SC. *In vitro* control of food-borne and food spoilage bacteria by essential oil and ethanol extracts of *Lonicera japonica* Thunb. *Food Chem*. 2009;116:670–675. doi:10.1016/j.foodchem.2009.03.014
12. Thanabhorn S, Jaijoy K, Thamaree S, Ingkaninan K, Panthong A. Acute and subacute toxicity study of the ethanol extract from *Lonicera japonica* Thunb. *J Ethnopharmacol*. 2006;107:370–373. doi:10.1016/j.jep.2006.03.023
13. Kuppusamy P, Yusoff MM, Maniam GP, Govindan N. Biosynthesis of metallic nanoparticles using plant derivatives and their new avenues in pharmacological applications-An updated report. *Saudi Pharm J*. 2016;24(4):473–484. doi:10.1016/j.jsps.2014.11.013
14. Patra JK, Das G, Fraceto LF, et al. Nano based drug delivery systems: recent developments and future prospects. *J Nanobiotechnol*. 2018;16(1):71. doi:10.1186/s12951-018-0392-8
15. Paul NS, Yadav RP, Kaul SK, Puri CP. A simple biogenic method for the synthesis of silver nanoparticles using syngonium podophyllum, an ornamental plant. *J Med Sci*. 2016;3:111–115. doi:10.5005/jp-journals-10036-1103
16. Durán N, Durán M, de Jesus MB, Seabra AB, Fávaro WJ, Nakazato G. Silver nanoparticles: a new view on mechanistic aspects on antimicrobial activity. *Nanomed Nanotechnol*. 2016;12(3):789–799. doi:10.1016/j.nano.2015.11.016
17. Pillai AM, Sivasankarapillai VS, Rahdar A, et al. Green synthesis and characterization of zinc oxide nanoparticles with antibacterial and antifungal activity. *J Mol Struct*. 2020;1211:128107. doi:10.1016/j.molstruc.2020.128107
18. Abhilash RK, Pandey BD. Microbial synthesis of iron-based nanomaterials—A review. *B Mater Sci*. 2011;34(2):191–198. doi:10.1007/s12034-011-0076-6
19. Ahmed S, Ahmad M, Swami BL, Ikram S. A review on plants extract mediated synthesis of silver nanoparticles for antimicrobial applications: a green expertise. *J Adv Res*. 2016;7(1):17–28. doi:10.1016/j.jare.2015.02.007
20. Zhang Y, Cheng X, Zhang Y, Xue X, Fu Y. Biosynthesis of silver nanoparticles at room temperature using aqueous aloe leaf extract and antibacterial properties. *Colloid Surface A*. 2013;423:63–68. doi:10.1016/j.colsurfa.2013.01.059
21. Park TJ, Lee KG, Lee SY. Advances in microbial biosynthesis of metal nanoparticles. *Appl Microbiol Biot*. 2016;100(2):521–534. doi:10.1007/s00253-015-6904-7
22. Yuan CG, Huo C, Yu S, Gui B. Biosynthesis of gold nanoparticles using Capsicum annuum var. grossum pulp extract and its catalytic activity. *Physica E*. 2017;85:19–26. doi:10.1016/j.physe.2016.08.010
23. Vo TS, Le TT, Kim SY, Ngo DH. The role of myricetin from *Rhodomyrtus tomentosa* (Aiton) Hassk fruits on downregulation of FceRI-mediated mast cell activation. *J Food Biochem*. 2020;44(3):e13143. doi:10.1111/jfbc.13143
24. Mendes RA, Almeida SKC, Soares IN, et al. A computational investigation on the antioxidant potential of myricetin 3,4'-di-O-alpha-L-rhamnopyranoside. *J Mol Model*. 2018;24(6):133. doi:10.1007/S00894-018-3663-2

25. López-Miranda JL, Vázquez M, Fletes N, Esparza R, Rosas G. Biosynthesis of silver nanoparticles using a Tamarix gallica leaf extract and their antibacterial activity. *Mater Lett*. 2016;176:285–289. doi:10.1016/j.matlet.2016.04.126
26. Vignesh V, Felix Anbarasi K, Karthikeyeni S, Sathiyanarayanan G, Subramanian P, Thirumurugan R. A superficial phyto-assisted synthesis of silver nanoparticles and their assessment on hematological and biochemical parameters in Labeo rohita (Hamilton, 1822). *Colloid Surface A*. 2013;439:184–192. doi:10.1016/j.colsurfa.2013.04.011
27. Xiong J, Li S, Wang W, Hong Y, Tang K, Luo Q. Screening and identification of the antibacterial bioactive compounds from *Lonicera japonica* Thunb. *leaves Food Chem*. 2013;138(1):327–333. doi:10.1016/j.foodchem.2012.10.127
28. Zhao Y. Study on antimicrobial effects of leaves extracts of *Lonicera japonica* Thunb. *Food Sci*. 2007;28(7):63–65. doi:10.1016/j.foodchem.2012.10.127
29. Park K, Park H, Nagappan A, et al. Polyphenolic compounds from Korean *Lonicera japonica* Thunb. induces apoptosis via AKT and caspase cascade activation in A549 cells. *Oncol Lett*. 2017;13(4):2521–2530. doi:10.3892/ol.2017.5771
30. Ge L, Xiao L, Wan H, et al. Chemical constituents from *Lonicera japonica* flower buds and their antihepatoma and anti-HBV activities. *Bioorg Chem*. 2019;92:103198. doi:10.1016/j.bioorg.2019.103198
31. Ge L, Lia J, Wan H, et al. Novel flavonoids from *Lonicera japonica* flower buds and validation of their anti-hepatoma and hepatoprotective activity in vitro studies. *Ind Crop Prod*. 2018;125:114–122. doi:10.1016/j.indcrop.2018.08.073